Cycloheptyl-fused NNO-ligands as electronically modifiable supports for M(II) (M = Co, Fe) chloride precatalysts; probing performance in ethylene oligo-/polymerization

Chantsalnyam Bariashir,[a,b] Zheng Wang,[a,b] Shizhen Du,[a] Gregory A. Solan,*[,a,c] Chuanbing Huang,[a,b] Tongling Liang,[a] and Wen-Hua Sun*[,a,b,d]

[a] Key Laboratory of Engineering Plastics and Beijing National Laboratory for Molecular Sciences, Institute of Chemistry, Chinese Academy of Sciences, Beijing 100190, China

[b] CAS Research/Education Center for Excellence in Molecular Sciences and International School, University of Chinese Academy of Sciences, Beijing 100049, China

[c] Department of Chemistry, University of Leicester, University Road, Leicester LE1 7RH, UK

[d] State Key Laboratory for Oxo Synthesis and Selective Oxidation, Lanzhou Institute of Chemical Physics, Chinese Academy of Sciences, Lanzhou 730000, China

Correspondence to: W.-H. Sun (E-mail: *whsun@iccas.ac.cn) or G. A. Solan (gas8@le.ac.uk*)

ABSTRACT: The N,N,O-cobalt(II), [2,3-{$C_4H_8C(NAr)$}:5,6-{$C_4H_8C(O)$}C_5HN]$CoCl_2$ (Ar = 2,6-$(CHPh_2)_2$-4-MeC_6H_2 **Co1**, 2,6-$(CHPh_2)_2$-4-EtC_6H_2 **Co2**, 2,6-$(CHPh_2)_2$-4-ClC_6H_2 **Co3**, 2,6-$(CHPh_2)_2$-4-FC_6H_2 **Co4**) and N,N,O-iron(II) complexes, [2,3-{$C_4H_8C(NAr)$}:5,6-{$C_4H_8C(O)$}C_5HN]$FeCl_2$ (Ar = 2,6-$(CHPh_2)_2$-4-MeC_6H_2 **Fe1**, 2,6-$(CHPh_2)_2$-4-EtC_6H_2 **Fe2**, 2,6-$(CHPh_2)_2$-4-ClC_6H_2 **Fe3**, 2,6-$(CHPh_2)_2$-4-FC_6H_2 **Fe4**), each containing one sterically enhanced but electronically modifiable N-2,6-dibenzhydryl-4-R^2-phenyl group, have been prepared by a one-pot template approach using α,α'-dioxo-2,3:5,6-bis(pentamethylene)pyridine, the corresponding aniline along with the respective cobalt or iron salt in acetic acid. Distorted square pyramidal geometries are the feature of the molecular structures of **Co1** – **Co4**. Upon activation with MAO or MMAO, **Co1** – **Co4** show good activities (up to 2.2 x 10^5 g mol^{-1}(Co) h^{-1}) affording short chain oligomers (C_4 – C_{30}) with good α-olefin selectivity. By contrast, **Fe1** – **Fe4**, in the presence of MMAO, displayed moderate activities (up 10.9 × 10^4 g(PE) mol^{-1}(Fe) h^{-1}) for ethylene polymerization forming low molecular weight linear polymers (up to 13.0 Kg mol^{-1}) incorporating saturated *n*-propyl and *i*-butyl chain ends. For both cobalt and iron, the pre-catalysts incorporating the more electron withdrawing 4-R^2-substituents [(Cl (**Co3**/**Fe3**), F (**Co4**/**Fe4**)] deliver the best catalytic activities, while with cobalt these types of substituents additionally broaden the oligomeric distribution.

KEYWORDS: α-Imino-α'-oxo-2,3:5,6-bis(pentamethylene)pyridine; Metal-Organic Catalysts; Coordination polymerization; Polyethylene; Oligomers.

INTRODUCTION

The mid to late 1990's saw some dramatic advances in late transition metal-based technology for ethylene oligo-/polymerization with reports of highly active iron and cobalt catalysts emerging towards the end of this period.[1-3] In particular, the bis(imino)pyridine-containing Fe(II) and Co(II) catalysts, first disclosed independently by Brookhart and Gibson, have attracted considerable interest over the years in both the academic and

industrial communities due to their remarkable activities for ethylene polymerization[1b,2] and their exceptional selectivities for ethylene oligomerization forming linear α-olefins.[3] As a consequence, a large number of investigations have been focused on ligand modification deriving from the parent bis(arylimino)pyridine framework (**A**, Chart 1). In the main these changes have been concerned with steric and electronic variations to the N-aryl groups[4] and to the substituents on the imine-carbon atoms.[2,5] Elsewhere, more dramatic structural changes have seen the development of 2,9-bis(imino)-1,10-phenanthrolines,[6] 2-benzimidazol-6-imino-pyridines,[7] N-((pyridin-2-yl)methylene)-8-amino quinolines[8] and 2,8-bis(imino)quinolines.[9] More recently, highly active iron and cobalt pre-catalysts bearing cycloalkyl-fused pyridine ligand sets such as, 1,8-diimino-2,3,4,5,6,7-hexahydroacridines,[10] 2-(1-arylimino)ethyl-8-arylimino-5,6,7-trihydroquinolines,[11] 2-(1-aryl iminoethyl)-9-arylimino-5,6,7,8-tetrahydrocyclo heptapyridines,[12] α,α'-bis(arylimino)-2,3:5,6-bis (pentamethylene)pyridines[13] (**B**, Chart 1) and 2-(arylimino)benzylidene-9-arylimino-5,6,7,8-tetrahydrocyclohepta[*b*]pyridylines[14] have been reported. On the other hand, lower activities were exhibited by the smaller ring cobalt complexes of 2-[1-(arylimino)ethyl]-7-arylimino-6,6-dimethylcyclopentapyridines.[15]

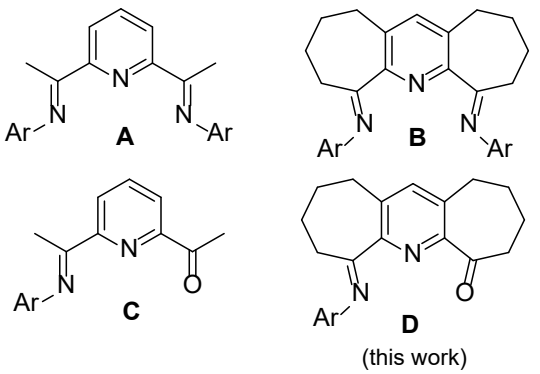

Chart 1 Ligand frameworks derived from bis(imino)pyridine, **A**

As an alternative to these tridentate nitrogen donor ligand sets, the N,N,O family represents another class of ligand that has seen some key developments within the polymerization arena. For example, 2-acetyl-6-arylimino-pyridines[16,17] (**C**, Chart 1), 2-(ethylcarboxylato)-6-iminopyridines,[18a] 2-imino-6-methanol-pyridines[18b] and 2-(benzimidazolyl)-6-(arylimino)pyridines[7a,c] have all been reported as ligand supports for active iron (and some cobalt) catalysts. Indeed, high activities in ethylene polymerization have been reported for iron complexes bearing the 2,6-diisopropylphenyl derivative of **C** (Chart 1).[16a] Furthermore, the chemistry of this ligand class with other divalent metal centers such as chromium, manganese and nickel has also been disclosed.[19]

In this work, we target a series of divalent iron and cobalt chloride complexes bearing the neutral N,N,O ligand, α-imino-α'-oxo-2,3:5,6-bis(pentamethylene)pyridine (**D**, Chart 1), in which the central pyridine is fused by two seven-membered rings with one α-position possessing an oxo group and the other a sterically bulky N-2,6-dibenzhydryl-4-R^2-phenyl group (R^2 = Me, Et, Cl, F). An in-depth investigation is initiated to explore the performance of these Fe(II) and Co(II) complexes as pre-catalysts in ethylene oligo-/polymerization with a view to ascertaining the most compatible co-catalyst, the role the metal center plays and the effect the electronic changes to the 4-R^2 substituent have on the ethylene chain growth. Full details of the synthesis and characterization for all complexes are also reported.

EXPERIMENTAL

General Considerations. All manipulations involving air- and moisture-sensitive compounds were carried out under nitrogen atmosphere using standard Schlenk techniques. Toluene was refluxed over sodium and distilled under nitrogen prior to use. Methylaluminoxane (MAO, 1.46 M solution in toluene) and modified methylaluminoxane (MMAO, 1.93 M in n-heptane) were purchased from Akzo Nobel Corp. High-purity ethylene was

purchased from Beijing Yansan Petrochemical Co. and used as received. Other reagents were purchased from Aldrich, Acros, or local suppliers. NMR spectra were recorded on a Bruker DMX 400 MHz instrument at ambient temperature using TMS as an internal standard; δ values were given in ppm and J values in Hz. FT-IR spectra were recorded on a Perkin-Elmer System 2000 FT-IR spectrometer. Elemental analysis was carried out using a Flash EA 1112 micro-analyzer. Molecular weights (M_w) and molecular weight distributions (MWD) of the polyethylenes were determined by Gel Permeation Chromatography using a PL-GPC220 instrument at 150 °C with 1,2,4-trichloro-benzene as the solvent. **Some mention of GC instrument and specification needed.** The thermograms for the crystallization and melt process were recorded using a differential scanning calorimeter (DSC, TA-Q2000) under a nitrogen atmosphere. Typically, a sample of about 5.0 mg was heated to 140 °C at a rate of 20 °C/min and kept for 2 min at 140 °C to remove the thermal history and then cooled at a rate of 20 °C/min to -40 °C. The ^{13}C NMR spectra of the polyethylenes were recorded on a Bruker DMX 300 MHz instrument at 135 °C in deuterated 1,1,2,2-tetrachloroethane-d_2 with TMS as an internal standard. The compounds, α,α'-dioxo-2,3:5,6-bis(pentamethylene)pyridine,[13b] 2,6-dibenzhydryl-4-methylbenzaniline, 2,6-dibenzhydryl-4-ethylaniline, 2,6-dibenzhydryl-4-chloroaniline and 2,6-dibenzhydryl-4-fluoroaniline were prepared using literature procedures.[20]

Synthesis of cobalt and iron complexes

Preparation of [2,3-{$C_4H_8C(NAr)$}:5,6-{$C_4H_8C(O)$}C_5HN]$CoCl_2$

Ar = 2,6-$(CHPh_2)_2$-4-MeC_6H_2) (Co1). A suspension of α,α'-dioxo-2,3:5,6-bis(penta-methylene)pyridine (0.243 g, 1.0 mmol), 2,6-dibenzhydryl-4-methylbenzaniline (1.776 g, 4.0 mmol) and $CoCl_2$ (0.13 g, 1.0 mmol) in glacial acetic acid (15 ml) was stirred and heated to reflux for 8 h. Diethyl ether was added to precipitate the solid, which was then filtered before being re-dissolved in methanol. The resulting methanol solution was concentrated to a minimum volume and diethyl ether added to precipitate the product. **Co1** was collected by filtration and dried under reduced pressure as a light green powder (0.497 g, 69%). FT-IR (KBr, cm^{-1}): 2943 (w), 2868 (w), 1651 ($\nu_{C=O}$, m), 1599 ($\nu_{C=N}$, s), 1552 (m), 1491 (s), 1448 (s), 1328 (m), 1254 (s), 1210 (m), 1167 (w), 1077 (m), 1031 (w), 969 (w), 922 (m), 857 (w), 798 (w), 767 (w), 701 (s). Anal. calc. for $C_{48}H_{44}Cl_2CoN_2O$ (794.7): C, 72.54; H, 5.58; N, 3.52. Found: C, 72.80; H, 5.45; N, 3.11.

Ar = 2,6-$(CHPh_2)_2$-4-EtC_6H_2 (Co2). Using a similar procedure and molar ratios to that described for **Co1** but with 2,6-dibenzhydryl-4-ethylaniline as the amine, **Co2** was obtained as a light green powder (0.62 g, 85%). FT-IR (KBr, cm^{-1}): 2937 (w), 2864 (w), 1655 ($\nu_{C=O}$, m), 1596 ($\nu_{C=N}$, s), 1548 (m), 1491 (s), 1448 (s), 1324 (m), 1253 (s), 1208 (m), 1171 (w), 1078 (m), 1029 (w), 969 (w), 923 (m), 863 (w), 794 (w), 766 (w), 700 (s). Anal. calc. for $C_{49}H_{46}Cl_2CoN_2O$ (808.74): C, 72.77; H, 5.73; N, 3.46. Found: C, 72.8; H, 5.45; N, 3.11.

Ar = 2,6-$(CHPh_2)_2$-4-ClC_6H_2 (Co3). Using a similar procedure and molar ratios to that described for **Co1** but with 2,6-dibenzhydryl-4-chloroaniline as the amine, **Co3** was obtained as a light green powder (0.38 g, 52%). FT-IR (KBr, cm^{-1}): 2938 (w), 2867 (w), 1647 ($\nu_{C=O}$, m), 1597 ($\nu_{C=N}$, s), 1550 (m), 1492 (s), 1446 (s), 1336 (m), 1258 (s), 1182 (m), 1138 (w), 1077 (m), 1030 (w), 962 (w), 919 (m), 863 (w), 792 (w), 766 (w), 700 (s). Anal. calc. for $C_{47}H_{41}Cl_3CoN_2O$ (815.13): C, 69.25; H, 5.07; N, 3.44. Found: C, 69.00; H, 4.93; N, 3.17.

Ar = 2,6-$(CHPh_2)_2$-4-FC_6H_2 (Co4). Using a similar procedure and molar ratios to that described for **Co1** but with 2,6-dibenzhydryl-4-fluoroaniline as the amine, **Co4** was obtained as a light green powder (0.14 g, 13%). FT-IR (KBr, cm^{-1}): 2970 (w), 2901 (w), 1647 ($\nu_{C=O}$, m), 1595 ($\nu_{C=N}$, s), 1550 (m), 1493 (s), 1447 (s), 1340 (m), 1257 (s), 1210 (m), 1187 (w), 1074 (m), 1038 (w), 1002 (w), 914 (m), 863 (w), 801 (w), 766

(w), 700 (s). Anal. calc. for $C_{47}H_{41}Cl_2CoFN_2O$ (798.68): C, 70.68; H, 5.17; N, 3.51. Found C, 71.04; H, 5.19; N, 3.42.

Preparation of [2,3-{$C_4H_8C(NAr)$}:5,6-{$C_4H_8C(O)$}C_5HN]$FeCl_2$

Ar = 2,6-$(CHPh_2)_2$-4-MeC_6H_2 (Fe1). A suspension of α,α'-dioxo-2,3:5,6-bis(pentamethylene) pyridine (0.243 g, 1.0 mmol), 2,6-dibenzhydryl-4-methylaniline (1.776 g, 4.0 mmol) and $FeCl_2{\cdot}4H_2O$ (0.199 g, 1.0 mmol) in glacial acetic acid (15 ml) was stirred and heated to reflux for 8 h. Diethyl ether was added to precipitate the solid, which was then filtered before being re-dissolved in methanol. The resulting methanol solution was concentrated to a minimum volume and diethyl ether added to precipitate the product. **Fe1** was collected by filtration and dried under reduced pressure as a blue powder (0.463 g, 65%). FT-IR (KBr, cm^{-1}): 2943 (w), 2868 (w), 1621 ($\nu_{C=O}$, m), 1591 ($\nu_{C=N}$, s), 1543 (w), 1493 (s), 1444 (s), 1321 (m), 1263 (m), 1179 (s), 1153 (w), 1077 (m), 1030 (w), 972 (w), 930 (m), 864 (w), 789 (w), 746 (w), 698 (s). Anal. calc. for $C_{48}H_{44}Cl_2FeN_2O$ (791.6): C, 72.83; H, 5.60; N, 3.54. Found: C, 73.07; H, 5.60; N, 3.48.

Ar = 2,6-$(CHPh_2)_2$-4-EtC_6H_2 (Fe2). Using a similar procedure and molar ratios to the described for **Fe1** but with 2,6-dibenzhydryl-4-ethylaniline as the amine, **Fe2** was obtained as a blue powder (0.70 g, 96%). FT-IR (KBr, cm^{-1}): 2934 (w), 2865 (w), 1633 ($\nu_{C=O}$, m), 1597 ($\nu_{C=N}$, m), 1553 (m), 1491 (s), 1447 (s), 1323 (m), 1257 (s), 1207 (m), 1166 (w), 1076 (w), 1031 (w), 970 (w), 923 (m), 863 (w), 804 (w), 768 (w), 698 (s). Anal. calc. for $C_{49}H_{46}Cl_2FeN_2O$ (805.65)**:** C, 73.05; H, 5.75; N, 3.48. Found C, 73.00; H, 5.75; N, 3.23.

Ar = 2,6-$(CHPh_2)_2$-4-ClC_6H_2 (Fe3). Using a similar procedure and molar ratios to the described for **Fe1** but with 2,6-dibenzhydryl-4-chloroaniline as the amine, **Fe3** was obtained as a blue powder (0.415 g, 57%). FT-IR (KBr, cm^{-1}): 2952 (w), 2871 (w), 1631 ($\nu_{C=O}$, m), 1593 ($\nu_{C=N}$, s), 1548 (m), 1493 (s), 1445 (s), 1326 (m), 1259 (s), 1181 (m), 1116 (w), 1077 (m), 1033 (w), 999 (w), 926 (m), 865 (w), 796 (w), 766 (w), 700 (s). Anal.

Table 1 Crystal data and structure refinement for **Co1**, **Co2**, **Co3** and **Co4**

	Co1	Co2	Co3	Co4
Empirical formula	$C_{48}H_{44}Cl_2CoN_2O$	$C_{49}H_{46}Cl_2CoN_2O$	$C_{47}H_{41}N_2OCl_3Co$	$C_{47}H_{41}Cl_2CoFN_2O$
F_w	794.68	808.71	815.10	798.7
T (K)	173.15 K	293(2) K	173.15 K	173.15 K
Wavelength	0.71073	0.71073	0.71073	0.71073
Crystal system	Orthorhombic	Orthorhombic	Orthorhombic	Orthorhombic
Space group	$Pna2_1$	$Pna2_1$	$Pna2_1$	$Pna2_1$
a(Å)	16.630(3)	16.615(3)	16.585(8)	16.760(3)
b(Å)	14.012(3)	14.087(3)	14.012(7)	14.016(3)
c(Å)	16.638(3)	16.935(3)	16.538(8)	16.289(3)
α(°)	90.00	90.00	90.00	90.00
β(°)	90.00	90.00	90.00	90.00
γ(°)	90.00	90.00	90.00	90.00
V(Å^3)	3877.0(13)	3964.0(14)	3843.0(3)	3826.5(13)
Z	4	4	4	4
D_{calcd} (mg m^3)	1.361	1.355	1.409	1.383
μ(mm^{-1})	0.621	0.608	0.695	0.633
F(000)	1660.0	1692.0	1692.0	1652.0
Crystal size (mm)	0.29×0.152×0.065	0.424×0.273×0.21	0.377×0.306×0.144	0.26×0.17×0.079
θ range (°)	1.900 - 27.471	2.245 - 27.480	6.220 - 55.240	3.788 -54.942
Limiting indices	-21<=h<=21 -18<=k<=18 -21<=l<=21	-21<=h<=21 -18<=k<=18 -21<=l<=21	-15 <= h <= 21 -18 <= k <= 17 -21 <= l <= 21	-21 <= h <= 21 -18 <= k <= 18 -21 <= l <= 21
No. of rflns collected	39989	40323	25274	50710
No. unique rflns [R(int)]	8704 (0.0463)	9015 (0.0314)	8752 (0.0817)	8708 (0.0544)
Completeness to θ (%)	99.5 %	99.4 %	98.0 %	100 %
Data/restraints/params	8704 / 1 / 488	9015 / 7 / 497	8752 / 1 / 488	8708 / 1 / 487
Goodness of fit on F^2	1.071	1.071	1.186	1.084
Final R indexes [I>=2σ (I)]	R_1 = 0.0396 wR_2 = 0.0852	R_1 = 0.0413 wR_2 = 0.1099	R_1 = 0.0780 wR_2 = 0.1438	R_1 = 0.0628 wR_2 = 0.1816

R indexes (all data)	R_1 = 0.0417 wR_2 = 0.0865	R_1 = 0.0418 wR_2 = 0.1104	R_1 = 0.0863 wR_2 = 0.1482	R1 = 0.0655 wR2 = 0.1927
Largest diff peak and hole (e Å^{-3})	0.283 and -0.253	1.261 and -0.424	0.400 and -0.340	2.190 and -0.670

calc. for $C_{47}H_{41}Cl_3FeN_2O$ (812.05): C, 69.52; H, 5.09; N, 3.45. Found: C, 69.00; H, 4.93; N, 3.17.

Ar = 2,6-$(CHPh_2)_2$-4-FC_6H_2 (Fe4). Using a similar procedure and molar ratios to the described for **Fe1** but with 2,6-dibenzhydryl-4-fluoroaniline as the amine, **Fe4** was obtained as a blue powder (0.24 g, 22%). FT-IR (KBr, cm^{-1}): 2940 (w), 2861 (w), 1645 ($\nu_{C=O}$, m), 1596 ($\nu_{C=N}$, m), 1546 (m), 1494 (m), 1445 (s), 1298 (w), 1258 (m), 1187 (m), 1080 (w), 1033 (w), 969 (w), 927 (w), 861 (w), 765 (w), 747 (w), 700 (s). Anal. calc. for $C_{47}H_{41}Cl_2FeFN_2O$ (795.6): C, 70.95; H, 5.19; N, 3.52. Found C, 70.53; H, 5.53; N 3.40.

X-ray crystallographic study

The single-crystal X-ray diffraction studies of **Co1**, **Co2**, **Co3** and **Co4** were carried out on a Rigaku sealed Tube CCD (Saturn 724+) diffractometer with graphite-monochromated Mo-Kα radiation (λ = 0.71073 Å) at 173(2) K with the exception of **Co2** at 293(2) K; cell parameters were obtained by global refinement of the positions of all collected reflections. Intensities were corrected for Lorentz and polarization effects and empirical absorption. The structures were solved by direct methods and refined by full-matrix least squares on F^2. All non-hydrogen atoms were placed in calculated positions. Structural solution and refinement were performed by using the SHELXTL-97 package.[21] The free solvents present within the single crystal were removed by using the SQUEEZE option of the crystallographic program PLATON.[22] Details of the X-ray refinements are provided in Table 1. CCDC 1564025 (**Co1**), 1564026 (**Co2**), 1564027 (**Co3**) and 1564028 (**Co4**) contain the crystallographic data for this article, which could be obtained free of charge from the Cambridge Crystallographic Data Centre via www.ccdc.cam.ac.uk/ data_request/cif.

RESULTS AND DISCUSSION

Synthesis and characterization.

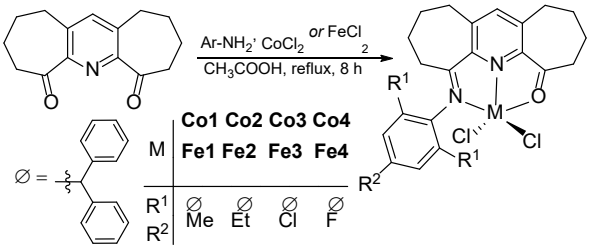

Scheme 1 Syntheses of **Co1** – **Co4** and **Fe1** – **Fe4**

The one-pot template reaction of α,α'-dioxo-2,3:5,6-bis(pentamethylene)pyridine, the corresponding metal halide ($CoCl_2$ or $FeCl_2{\cdot}4H_2O$) and the targeted aniline in acetic acid at reflux gave, on work-up, [2,3-{C_4H_8C(NAr)}:5,6-{C_4H_8C(O)}C_5HN]$CoCl_2$ (Ar = 2,6-$(CHPh_2)_2$-4-MeC_6H_2 **Co1**, 2,6-$(CHPh_2)_2$-4-EtC_6H_2 **Co2**, 2,6-$(CHPh_2)_2$-4-ClC_6H_2 **Co3**, 2,6-$(CHPh_2)_2$-4-FC_6H_2 **Co4**) and [2,3-{C_4H_8C(NAr)):5,6-(C_4H_8C(O)}C_5HN]$FeCl_2$ (Ar = 2,6-$(CHPh_2)_2$-4-MeC_6H_2 **Fe1**, 2,6-$(CHPh_2)_2$-4-EtC_6H_2 **Fe2**, 2,6-$(CHPh_2)_2$-4-ClC_6H_2 **Fe3**, 2,6-$(CHPh_2)_2$-4-FC_6H_2 **Fe4**) in moderate to good yields (13 – 96%) (Scheme 1).[10,13,14] The yields for **Co4** and **Fe4** fall at the lower end of the yield range and this can be attributed to their increased solubility in methanol, the solvent used for recrystallization. All the cobalt complexes are air and moisture stable, while in solution the iron complexes proved susceptible to oxidation on exposure to the air over a few minutes; in the solid state, however, the iron complexes are air stable. Complexes **Co1** – **Co4** and **Fe1** – **Fe4** have been characterized by infra-red spectroscopy and microanalyses, while all four cobalt complexes have been the subject of single crystal X-ray diffraction studies.

Single crystals of **Co1**, **Co2**, **Co3** and **Co4** suitable for the X-ray determinations were grown by slow diffusion of diethyl ether into a

dichloromethane solution of the corresponding complex at room temperature. Perspective views of **Co1**, **Co2**, **Co3** and **Co4** are shown in Figures 1 – 4; selected bond distances and angles are compiled in Table 2. The four structures are similar and will be discussed together. Each structure consists of a cobalt center surrounded by two nitrogen and one

Table 2 Selected lengths (Å) and angles (Å) for **Co1** - **Co4**

	Co1	Co2	Co3	Co4
		Bond lengths (Å)		
Co(1)-N(1)	2.059(3)	2.050(2)	2.050(4)	2.068(4)
Co(1)-N(2)	2.161(3)	2.151(3)	2.166(4)	2.154(5)
Co(1)-O(1)	2.280(3)	2.276(3)	2.266(4)	2.255(5)
Co(1)-Cl(1)	2.2344(11)	2.2686(11)	2.2328(18)	2.2832(17)
Co(1)-Cl(2)	2.2699(11)	2.2358(11)	2.2709(17)	2.2376(18)
C(1)-O(1)	1.219(4)	1.217(4)	1.222(6)	1.228(8)
N(1)-C(14)	1.339(4)	1.333(4)	1.352(7)	1.329(7)
N(1)-C(15)	1.347(4)	1.346(4)	1.336(7)	1.333(7)
N(2)-C(13)	1.293(4)	1.295(4)	1.296(6)	1.291(7)
N(2)-C(16)	1.438(4)	1.441(4)	1.425(6)	1.443(7)
		Bond angles (°)		
N(1)-Co(1)-N(2)	75.84(11)	76.19(11)	75.82(17)	75.24(18)
N(1)-Co(1)-O(1)	73.50(10)	73.97(10)	73.81(16)	73.06(17)
N(2)-Co(1)-O(1)	145.93(10)	147.26(11)	145.86(15)	142.77(19)
Cl(1)-Co(1)-Cl(2)	122.53(5)	123.21(5)	121.83(7)	118.08(8)
N(2)-Co(1)-Cl(1)	101.09(8)	106.08(8)	100.32(12)	103.74(14)
N(2)-Co(1)-Cl(2)	105.81(8)	100.64(8)	105.90(12)	102.54(14)
Cl(2)-Co(1)-O(1)	92.23(8)	92.02(8)	93.01(12)	94.59(14)
Cl(1)-Co(1)-O(1)	92.64(7)	91.37(9)	93.00(11)	96.63(16)
O(1)-C(1)-C(2)	121.5(3)	121.2(3)	121.9(5)	122.2(6)
C(1)-O(1)-Co(1)	114.1(2)	113.7(2)	114.2(4)	114.6(4)

oxygen donor atom belonging to the N,N,O-ligand as well as two chloride ligands to complete a five coordinate geometry. The main difference between the structures arises in the substituent located at *para*-position of the N-aryl group [Me (**Co1**), Et (**Co2**), Cl (**Co3**), F (**Co4**)]. Closer inspection of the geometry reveals that it can be best described as distorted square-pyramidal,[2,13,17,19] in which two nitrogen, one oxygen and one chloride atom form the basal plane with the second chloride occupying the apical position. This type of geometry can be further justified by determination of the tau value (τ) in which a value of zero defines a perfect square pyramid and unity a perfect trigonal bipyramid; the results are given in Table 3.[23] For all four structures, the τ value lies between 0.39 and 0.41 indicative of a distorted square planar geometry. There are some differences in the bond lengths involving the N,N,O ligand with the distances generally following the order: Co-O [2.255(5) - 2.280(3) Å] > Co-N_{imine} [2.151(3) - 2.166(4) Å] > Co-$N_{pyridine}$ [2.050(2) - 2.068(4) Å]. No discernable effect on the Co-N_{imine} distances between structures can be detected on varying the *para*-substituent on the N-aryl group. As with related cobalt(II) complexes containing a pyridine-based tridentate ligands, the central Co-$N_{pyridine}$ distance is the shortest highlighting its more effective interaction.[10,13b] The variation in the exterior Co-N_{imino} and Co-O bond lengths can be attributed to the borderline cobalt(II) ion having preference for bonding with the softer imine donor; similar asymmetry has been seen in related N,N,O-M(II) complexes.[16,17,19] The N,N,O-coordination plane is almost perpendicular to the N-aryl ring with the dihedral angles of 88.64° (**Co1**), 87.84° (**Co2**), 88.51° (**Co3**) and 83.84° (**Co4**).

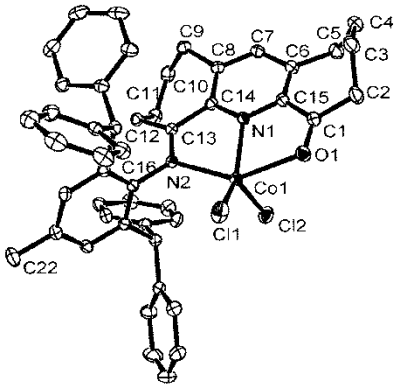

Fig. **1** ORTEP representation of **Co1** with the thermal ellipsoids at the 30% probability level; hydrogen atoms have been omitted for clarity.

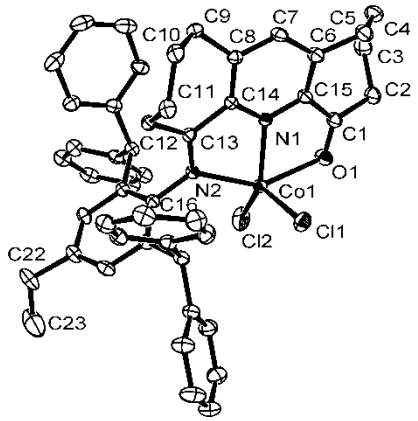

Fig. 2 ORTEP representation of **Co2** with the thermal ellipsoids at 30% probability level; hydrogen atoms have been omitted for clarity.

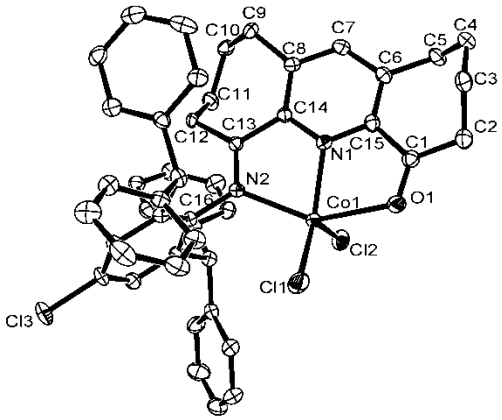

Fig. 3 ORTEP representation of **Co3** with the thermal ellipsoids at the 30% probability level; hydrogen atoms have been omitted for clarity.

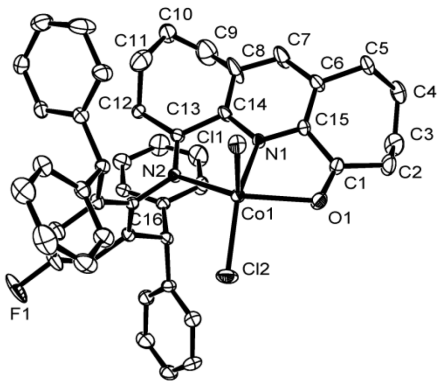

Fig. 4 ORTEP representation of **Co4** with thermal ellipsoids at the 30% probability level; hydrogen atoms have been omitted for clarity.

Table 3 Geometric tau value (τ) parameter

Complex	α (°)	β (°)	τ^a
Co1	122.53	145.93	0.39
Co2	123.21	147.26	0.4
Co3	121.83	145.86	0.4
Co4	118.08	142.77	0.41

[a]τ = (β - α)/ where β is the largest angle and α the second largest.[23]

In the FT-IR spectra, all the complexes exhibit a carbonyl band around 1650 cm^{-1} while the imine band can be seen at lower wavenumber around 1595 cm^{-1}. These distinct stretching frequencies for the bound C=O and C=N groups resemble those observed for the corresponding ones in [2-acetyl-6-{1-((2,6-diisopropylphenyl)imino)ethylpyridine]-cobalt(II) and -iron(II) chlorides.[17,18b] The microanalytical data for the complexes is consistent with the elemental composition proposed.

Catalytic evaluation of the metal complexes

Using Co1 – Co4. With the aim to explore the capacity of **Co1** – **Co4** to promote the oligomerization and/or polymerization of ethylene, we set about establishing the most suitable co-catalyst to deliver the best catalytic activity for the particular process. In the first instance **Co3** was employed as the test pre-catalyst with various aluminum-based co-

catalysts including modified methylaluminumoxane (MMAO), methylaluminumoxane (MAO), diethylaluminum chloride (Et_2AlCl), ethylaluminum sesquichloride (EASC), triethylaluminum (Et_3Al) and trimethylaluminum (TMA). A typical test was performed at 30 °C, under 10 atmospheres of ethylene pressure over a reaction time of 30 minutes using toluene as the solvent; the results are presented in Table 4.

Firstly, using **Co3** in combination with 1000 equivalents of MMAO or MAO as co-catalysts, only low activities (10^4 g mol^{-1} h^{-1}) were observed for ethylene polymerization generating low molecular weight materials (entries 1 and 2, Table 4). With TMA as co-catalyst only a trace amount of polymer was obtained while the other co-catalysts gave no evidence for any polymeric material. On the other hand, **Co3**/MMAO and **Co3**/MAO showed much higher activities for ethylene oligomerization ($1.14 - 2.08 \times 10^5$ g mol^{-1} h^{-1}) affording short chain olefins in the C_4-C_{30} range (entries 1 and 2, Table 4).

Table 4 Co-catalyst screen using **Co3** as pre-catalyst

Entry[a]	Co-cat.	T, °C	Al/Co	Oligom. activity[b]	Oligom. distribution	Polym. activity[c]	T_m[d], °C	M_w[e]	M_w/M_n[e]
1	MMAO	30	1000	2.08	C_4-C_{30}	3.4	126.7	7.8	8.4
2	MAO	30	1000	1.14	C_4-C_{30}	6.4	125.2	10.2	8.9
3	$AlEt_2Cl$	30	200	-	-	-	-	-	-
4	EASC	30	200	-	-	-	-	-	-
5	TMA	30	200	trace	-	-	-	-	-
6	$AlEt_3$	30	200	-	-	-	-	-	-

[a] Reaction conditions: 5 µmol of **Co3**; 30 minutes; 10 atmospheres of ethylene; 30 °C; 100 ml of toluene. [b] In units of 10^5 g mol^{-1}(Co) h^{-1}. [c] In units of 10^4 g(PE) mol^{-1}(Co) h^{-1}. [d] Determined by DSC. [e] M_w: kg mol^{-1}, M_w and M_w/M_n determined by GPC.

To optimize the conditions of the **Co3**-mediated ethylene oligomerization, MAO and MMAO were selected as the co-catalysts for a more detailed study of the reaction conditions, linked to the molar ratio of co-catalyst/pre-catalyst and reaction temperature with the pressure of ethylene maintained at 10 atmospheres; the results are collected in Tables 5 and 6.

On activation with MAO, **Co3** displayed a peak in catalytic activity (1.14×10^5 g mol^{-1} h^{-1}) at an Al/Co molar ratio of 1000 (entry 1, Table 5), while increasing the ratio in increments of 500 up to 2500 shows a steady drop in the activity. By contrast, when MMAO was employed as co-catalyst and the Al/Co molar ratio changed from 1000 to 2500, the catalytic activity of **Co3** reached a maximum (2.22×10^5 g mol^{-1} h^{-1}) at an Al/Co molar ratio of 1500 (entry 2, Table 6). Indeed, this activity (entry 2, Table 6) is almost double that observed using MAO as co-catalyst. Using the more efficient **Co3**/MMAO catalyst, with the Al/Co molar ratio fixed at 1500, the reaction temperature was raised from 30 to 70 °C with the result that the activity rapidly dropped from its maximum at 30 °C (entries 2, 9-11, Table 6); this observation is likely due to decomposition of the active species at higher temperature and possibly the poorer solubility of ethylene in toluene as this higher temperature.[7a,b, 18a] A similar finding was observed when the temperature of the run for **Co3**/MAO was raised from 30 to 40 °C (entries 1 and 5, Table 5).

With the optimal conditions established for **Co3** [MMAO as co-catalyst, Al/Co ratio = 1500,

temperature = 30 °C], the remaining cobalt complexes **Co1**, **Co2** and **Co4** were investigated under the same conditions. Like **Co3**, all the complexes were active for ethylene oligomerization with their activities falling in the range 2.22 – 0.37 g mol^{-1} h^{-1} with the relative ranking being **Co3** (Cl) > **Co4** (F) > **Co2** (Et) > **Co1** (Me) (entries 2, 9-11, Table 6).

Table 5 Ethylene oligomerization by **Co3**/MAO

Entry[a]	Pre-cat.	Co-cat.	Al/Co	T, °C	Act.[b]	Oligomer distribution (%)[c]					
						$C_4/\sum C$	$C_6/\sum C$	$C_8/\sum C$	$C_{10-14}/\sum C$	$C_{16-30}/\sum C$	α-olefin
1	**Co3**	MAO	1000	30	1.14	24.7	15.9	12.2	20.5	26.6	100
2	**Co3**	MAO	1500	30	0.96	20.2	15.2	12.3	25.2	27.1	96
3	**Co3**	MAO	2000	30	0.95	16.2	16.2	12.1	27.5	28.0	99
4	**Co3**	MAO	2500	30	0.83	24.0	16.8	9.6	24.0	25.6	98
5	**Co3**	MAO	1000	40	0.27	28.2	5.1	3.8	14.1	48.8	100

[a] Conditions: 5 µmol of Co pre-catalyst; 30 minutes; 10 atmospheres of ethylene; 100 ml toluene. [b] In units of 10^5 g mol^{-1} h^{-1}. [c] Determined by GC; ∑C signifies the total amount of oligomers.

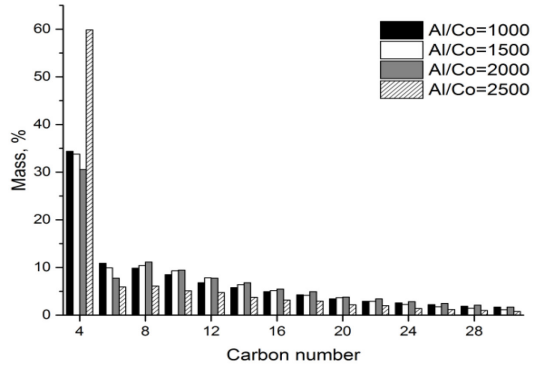

Fig. 5 Oligomer distribution displayed by **Co3**/MMAO with different Al/Co ratios (entries 1 - 4, Table 5).

Clearly, the nature of the 4-R^2 substituent on the N-aryl group affects the catalytic performance with the more electron withdrawing groups favoring higher activity.[4f, 24] With regard to the oligomer distribution, **Co3** and **Co4** show a high selectivity for α-olefins in the range C_4-C_{30} (entries 2 and 11, Table 6), while for **Co1** and **Co2** the range is narrower falling between C_4 and C_8 (entries 9 and 10, Table 6). In general, 1-butenes constitute the predominant fraction of all the distributions; this observation is illustrated in Figure 6 for **Co3**/MMAO conducted with different Al/Co molar ratios. A similar preference for 1-butenes has been noted for some bis(imino)pyridine-cobalt catalysts.[6f,7a-d]

Using Fe1 – Fe4. Based on previous findings for iron catalysts, high activities tend to be obtained using the methylaluminoxane-type co-catalysts and in particular MMAO.[11a, 12a, 13a, 14b] Hence, MMAO was selected as co-catalyst and **Fe4** chosen as the test pre-catalyst using toluene as the solvent and the ethylene pressure fixed at 10 atmospheres; optimization studies exploring variations in Al/Fe molar ratio and reaction temperature are discussed below while the results of the polymerization runs are collected in Table 7.

On changing the Al/Fe molar ratio from 1000 to 3000 for **Fe4**/MMAO (entries 1-5, Table 7) with the temperature maintained at 30 °C, the maximum activity for the polymerizations was 8.8×10^4 g(PE) mol^{-1}(Fe) h^{-1} obtained with an Al/Fe ratio of 2500 (entry 4, Table 7). Unlike with **Co3**, inspection of the gas chromatograph of the reaction solution revealed no evidence for oligomeric material being generated. Increasing the Al/Fe molar ratio from 2500 to 3000, the activity was found to sharply decrease. It is worth mentioning that the

highest activity recorded in this study is comparatively low

Table 6 Ethylene oligomerization using **Co3**/MMAO

						Oligomer distribution (%)[c]					
Entry[a]	Pre-cat.	Co-cat.	Al/Co	T, °C	Act.[b]	$C_4/\sum C$	$C_6/\sum C$	$C_8/\sum C$	$C_{10-14}/\sum C$	$C_{16-30}/\sum C$	α-olefin
1	**Co3**	MMAO	1000	30	2.08	34.4	11.0	9.8	21.0	23.8	83.5
2	**Co3**	MMAO	1500	30	2.22	33.8	9.9	10.4	23.5	22.4	83.7
3	**Co3**	MMAO	2000	30	1.89	30.6	7.7	11.1	24.0	26.6	85.0
4	**Co3**	MMAO	2500	30	1.83	59.8	5.9	6.1	13.6	14.5	79.0
5	**Co3**	MMAO	1500	40	0.90	78.7	4.8	4.7	4.3	7.4	75.2
6	**Co3**	MMAO	1500	50	0.75	83.2	8.1	5.0	1.3	2.3	63.0
7	**Co3**	MMAO	1500	60	0.53	78.8	1.3	8.6	4.6	6.6	64.2
8	**Co3**	MMAO	1500	70	0.43	83.3	5.0	11.4	-	-	80.0
9	**Co1**	MMAO	1500	30	0.37	89.6	4.7	5.7	-	-	82.0
10	**Co2**	MMAO	1500	30	0.54	93.6	2.6	3.8	-	-	63.5
11	**Co4**	MMAO	1500	30	0.86	70.4	5.3	7.4	7.0	9.8	74.0

[a] Conditions: 5 µmol of cobalt pre-catalyst; 30 minutes; 10 atmospheres of ethylene; 100 ml toluene. [b] In units of 10^5 g mol^{-1}(Co) h^{-1}. [c] Determined by GC; ∑C signifies the total amount of oligomers.

Table 7 Ethylene polymerization using **Fe1 - Fe4**/MMAO

Entry[a]	Pre-cat.	Co-cat	T, °C	Al/Fe	PE/g	Act.[b]	T_m[c], °C	M_w[d]	M_w/M_n[d]
1	**Fe4**	MMAO	30	1000	0.06	2.4	128.9	13.0	3.5
2	**Fe4**	MMAO	30	1500	0.15	6.4	128.6	10.8	3.5
3	**Fe4**	MMAO	30	2000	0.173	6.9	128.3	9.8	3.8
4	**Fe4**	MMAO	30	2500	0.219	8.8	128.2	12.7	5.7
5	**Fe4**	MMAO	30	3000	0.093	3.72	127.1	9.6	5.9
6	**Fe4**	MMAO	40	2500	trace	-	-	-	-
7	**Fe1**	MMAO	30	2500	trace	-	-	-	-
8	**Fe2**	MMAO	30	2500	trace	-	-	-	-
9	**Fe3**	MMAO	30	2500	0.273	10.9	125.1	6.4	4.8

[a] Conditions: 5 µmol of Fe pre-catalyst; 30 minutes; 10 atmospheres of ethylene; 100 ml of toluene. [b] In units of 10^4 g(PE) mol^{-1}(Fe) h^{-1}. [c] Determined by DSC. [d] M_w: kg mol^{-1}, M_w and M_w/M_n determined by GPC.

when put alongside the data reported for structurally related iron pre-catalysts bearing 2-acetyl-6-iminopyridines (**C**) and α,α'-bis(arylimino)-2,3:5,6-bis(pentamethylene)-pyridines (**B**).[16a,13a] This may be steric in origin as these previous studies employed less hindered N-aryl groups when compared with the bulky N-

2,6-dibenzhydryl-4-R^2-phenyl group used herein.[7b] With regard to the molecular weight of the polymers, the overall trend is to lower as the Al/Fe ratio is increased, although the run using 2500 molar equivalents of MMAO shows some apparent anomalous behavior (entry 4, Table 7). The resultant polyethylenes are all of low molecular weight with the highest of the series being 13.0 Kg mol^{-1} which was generated with an Al/Fe ratio of 1000; the GPC curves shown in Figure 6 illustrate these molecular weight variations. With the Al/Fe molar ratio fixed at 2500, the temperature of the polymerization using **Fe4**/MMAO was raised from 30 to 40 °C. However, a dramatic drop in catalyst performance resulted with only trace amounts of polymer detectable at this higher temperature (entry 6, Table 7). This fall-off in activity can be attributed to the lower thermal stability of the active species, as well as lower solubility of ethylene monomer in toluene at elevated temperature.[13b, 15a]

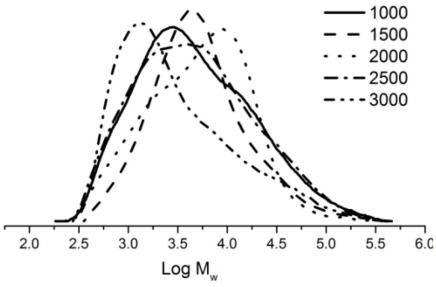

Fig. 6 GPC curves for the polyethylenes obtained with **Fe4**/MMAO with various Al/Fe various (entries 1-5, Table 6)

With the optimal conditions established for **Fe4**/MMAO [Al/Fe molar ratio = 2500, reaction temperature = 30 °C), **Fe1**, **Fe2** and **Fe3** were all evaluated using these conditions (entries 7-9, Table 7). While **Fe1** and **Fe2** gave only trace quantities of polymer, **Fe3** proved to be the most active of the four iron pre-catalysts displaying an activity of 10.9 × 10^4 g(PE) mol^{-1}(Fe) h^{-1} and affording low molecular weight polyethylene with relatively narrow molecular weight distribution (M_w = 6.4 Kg mol^{-1}, M_w/M_n = 4.8). As with the cobalt pre-catalysts, **Co1** – **Co4**, the nature of the 4-R^2-substituent on the N-aryl group has a noticeable effect on the polymerization performance. It is evident that electron withdrawing groups [Cl (**Fe3**), F (**Fe4**)] have a positive effect on the catalytic activity for the polymerization, while electron donating groups [Me (**Fe1**), Et (**Fe2**)] the opposite (entries 4, 7-9, Table 7).

To explore the microstructural properties of the polyethylene, a sample of the polymer obtained with **Fe3**/MMAO at 30 °C (entry 9, Table 7) was characterized using high temperature ^{13}C NMR spectroscopy (recorded at 135 °C in deuterated 1,1,2,2-tetrachloroethane-d_2). A peak of high intensity around δ 30.2 in the ^{13}C NMR spectrum confirms the high linearity of the polyethylene obtained (Figure 7),[13a,b, 16a] which is further evidenced by its high melting temperature (T_m = 125.1 °C, entry 9, Table 7).[13a]

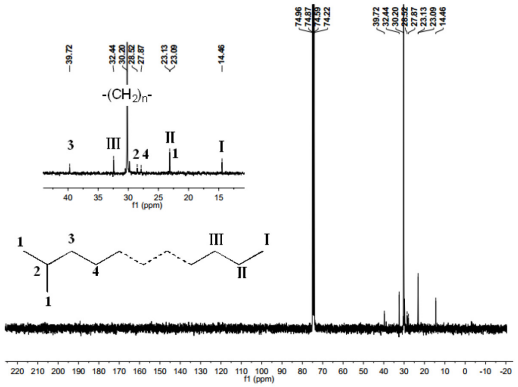

Fig. 7 ^{13}C NMR spectrum of the polyethylene obtained using **Fe3**/MMAO at 30 °C (entry 9, Table 7); expansion shows the aliphatic region

In addition, peaks at δ 39.72, 28.52, 27.87 and 23.09 can be ascribed to an *iso*-butyl end-group (peaks 1 - 4 in Figure 7), while the signals at δ 32.44, 23.13 and 14.46 to an *n*-propyl end-group (peaks I - III in Figure 7).[25] Interestingly, no evidence of unsaturated chain ends could be detected hence precluding chain termination via β-H elimination. Given the presence of an *iso*-butyl end-group, it would seem probable that these catalyst systems undergo termination by chain transfer to aluminum and in particular to Al(i-Bu)$_3$ and its derivatives (*e.g.*,

i-Bu_2AlMe) present in MMAO. Indeed, a mechanism of this type has recently been proposed by Bryliakov *et al.* to account for a similar iso-butyl/n-propyl chain-end combination which occurs at high concentrations of MMAO using bis(imino)pyridine-iron catalysts.[25] Related linear polyethylenes are expected for the other samples prepared in this study and indeed the melting temperatures of between 127.1 – 128.9 ^{o}C support this (entries 1-5, Table 7).

Conclusions

A one-pot synthetic route to a series of ring-fused N,N,O-cobalt(II) (**Co1** – **Co4**) and N,N,O-iron(II) (**Fe1** – **Fe4**) chloride complexes, each incorporating a sterically bulky N-2,6-dibenzhydryl-4-R^2-phenyl group at the α-position of one of the two fused 7-membered rings, has been successfully developed. The 4-R^2 substituent on the N-aryl group has been systematically modified to include both electron withdrawing [F (**Co4**/**Fe4**), Cl (**Co3**/**Fe3**)] and electron donating groups [CH_3 (**Co1**/**Fe1**), CH_2CH_3 (**Co2**/**Fe3**)). For the cases of **Co1**, **Co2**, **Co3** and **Co4**, their structures have been determined by X-ray diffraction. In the presence of MMAO, **Co1** – **Co4** exhibited good activities for ethylene oligomerization with **Co3** the highest [1.83 - 2.22 × 10^5 g mol^{-1}(Co) h^{-1}] generating α-olefins (C_4-C_{30}) with good selectivity. Conversely, **Fe1** – **Fe4** displayed moderate activities for ethylene polymerization forming low molecular weight highly linear polymer containing saturated *n*-propyl and *i*-butyl chain ends. The electronic properties of the 4-R^2-substituent have a notable effect on catalytic performance with higher activities observable for both the iron and cobalt pre-catalysts containing electron withdrawing substituents (R^2 = Cl, F); these types of R^2 substituent also have the effect of broadening the oligomer distribution for cobalt.

Acknowledgements

This work was supported by the National Natural Science Foundation of China (Nos. 21374123 and U1362204). CB is grateful to the CAS-TWAS president's fellowship. GAS thanks the Chinese Academy of Sciences for a Visiting Fellowship.

References

1. (a) L. K. Johnson, C.M. Killian, M. Brookhart, *J. Am. Chem. Soc*., 1995, 117, 6414–6415; (b) B. L. Small, M. Brookhart, *J. Am. Chem. Soc*., 1998, 120, 4049–4050.
2. (a) G. J. P. Britovsek, V. C. Gibson, B. S. Kimberley, P. J. Maddox, S. J. McTavish, G. A. Solan, A. J. P. White, D. J. Williams, *Chem. Commun*., 1998, 849–850; (b) G. J. P. Britovsek, M. Bruce, V. C. Gibson, B. S. Kimberley, P. J. Maddox, S. Mastroianni, S. J. McTavish, C. Redshaw, G. A. Solan, S. Strömberg, A. J. P. White, D. J. Williams, *J. Am. Chem. Soc*., 1999, 121, 8728–8740.
3. (a) B. L. Small, M. Brookhart, *J. Am. Chem. Soc*., 1998, 120, 7143–7144; (b) G. J. P. Britovsek, S. Mastroianni, G. A. Solan, S. P. D. Baugh, C. Redshaw, V. C. Gibson, A. J. P. White, D. J. Williams, M. R. J. Elsegood, *Chem. Eur. J*., 2000, 6, 2221–2231.
4. (a) G. J. P. Britovsek, V. C. Gibson, B. S. Kimberley, S. Mastroianni, C. Redshaw, G. A. Solan, A. J. P. White, D. J. Williams, *J. Chem. Soc, Dalton Trans*., 2001, 1639–1644; (b) J. Yu, H. Liu, W. Zhang, X. Hao, W.-H. Sun, *Chem Commun*., 2011, 47, 3257–3259; (c) J. Yu, W. Huang, L. Wang, C. Redshaw, W.-H. Sun, *Dalton Trans*., 2011, 40, 10209–10214; (d) S. Wang, B. Li, T. Liang, C. Redshaw, Y. Li, W.-H. Sun, *Dalton Trans*., 2013, 42, 9188–9197; (e) W. Zhao, J. Yu, S. Song, W. Yang, H. Liu, X. Hao, C. Redshaw, W.-H. Sun, *Polymer*, 2012, 53, 130–137; (f) X. Cao, F. He, W. Zhao, Z. Cai, X. Hao, T. Shiono, C. Redshaw, W.-H. Sun, *Polymer*, 2012, 53, 1870–1880; (g) F. He, W. Zhao, X.-P. Cao, T. Liang, C. Redshaw, W.-H. Sun, *J. Organomet. Chem*., 2012, 713, 209–216; (h) J. Lai, W. Zhao, W. Yang, C. Redshaw, T. Liang, Y. Liu, W.-H. Sun, *Polym. Chem*., 2012, 3, 787–793; (i) W.-H. Sun, W. Zhao, J. Yu, W. Zhang, X. Hao, C. Redshaw,

Macromol. Chem. Phys., 2012, 213, 1266–1273; (j) W. Zhang, S. Wang, S. Du, C.-Y. Guo, X. Hao, W.-H. Sun, *Macromol. Chem. Phys*., 2014, 215, 1797–1809; (k) E. Yue, Y. Zeng, W. Zhang, Y. Sun, X.-P. Cao, W.-H. Sun, *Sci. China Chem*., 2016, 59, 1291–1300; (l) W. Zhao, E. Yue, X. Wang, W. Yang, Y. Chen, X. Hao, X. Cao, W.-H. Sun, *J. Polym. Sci., Part A: Polym. Chem*., 2017, 55, 988–996.

5. (a) S. McTavish, G. J. P. Britovsek, T. M. Smit, V. C. Gibson, A. J. P. White, D. J. Williams, *J. Mol. Catal. A: Chem*., 2007, 261, 293–300; (b) T. M. Smit, A. K. Tomov, G. J. P. Britovsek, V. C. Gibson, A. J. P. White, D. J. Williams, *Catal. Sci. Technol*., 2012, 2, 643–655.
6. (a) L. Wang, W.-H. Sun, L. Han, H. Yang, Y. Hu, X. Jin, *J. Organomet. Chem*., 2002, 658, 62–70. (b) W.-H. Sun, S. Jie, S. Zhang, W. Zhang, Y. Song, H. Ma, *Organometallics*, 2006, 25, 666–677; (c) J. D. A. Pelletier, Y. D. M. Champouret, J. Cardarso, L. Clowes, M. Gañete, K. Singh, V. Thanarajasingham, G. A. Solan, *J. Organomet. Chem*., 2006, 691, 4114–4123; (d) S. Jie, S. Zhang, K. Wedeking, W. Zhang, H. Ma, X. Lu, Y. Deng, W.-H. Sun, *C. R. Chim*., 2006, 9, 1500–1509; (e) S. Jie, S. Zhang, W.-H. Sun, X. Kuang, T. Liu, J. Guo, *J. Mol. Cat. A: Chem*., 2007, 269, 85–96; (f) S. Jie, S. Zhang, W.-H. Sun, *Eur. J. Inorg. Chem*., 2007, 5584–5598.
7. (a) W.-H. Sun, P. Hao, S. Zhang, Q. Shi, W. Zuo, X. Tang, *Organometallics*, 2007, 26, 2720–2734; (b) Y. Chen, P. Hao, W. Zuo, K. Gao, W.-H. Sun, *J. Organomet. Chem*., 2008, 693, 1829–1840; (c) L. Xiao, R. Gao, M. Zhang, Y. Li, X. Cao, W.-H. Sun, *Organometallics*, 2009, 28, 2225–2233; (d) R. Gao, Y. Li, F. Wang, W.-H. Sun, M. Bochman, *Eur. J. Inorg. Chem*., 2009, 4149–4156.
8. K. Wang, K. Wedeking, W. Zuo, D. Zhang, W.-H. Sun, *J. Organomet. Chem*., 2008, 693, 1073–1080.
9. S. Zhang, W.-H. Sun, T. Xiao, X. Hao, *Organometallics*, 2010, 29, 1168–1173.
10. V. K. Appukuttan, Y. Liu, B. C. Son, C.-S. Ha, H. Suh, I. Kim, *Organometallics*, 2011, 30, 2285–2294.
11. (a) W. Zhang, W. Chai, W.-H. Sun, X. Hu, C. Redshaw, X. Hao, *Organometallics*, 2012, 31, 5039–5048; (b) W.-H. Sun, S. Kong, W. Chai, T. Shiono, C. Redshaw, X. Hu, C. Guo, X. Hao, *Appl. Catal. A*., 2012, 447–448, 67–73.
12. (a) F. Huang, Q. Xing, T. Liang, Z. Flisak, B. Ye, X. Hu, W. Yang, W.-H. Sun, *Dalton Trans*., 2014, 43, 16818–16829; (b) F. Huang, W. Zhang, E. Yue, T. Liang, X. Hu, W.-H. Sun, *Dalton Trans*., 2016, 45, 657–666.
13. (a) S. Du, X. Wang, W. Zhang, Z. Flisak, Y. Sun, W.-H. Sun, *Polym. Chem*., 2016, 7, 4188–4197; (b) S. Du, W. Zhang, E. Yue, F. Huang, T. Liang, W.-H. Sun, *Eur. J. Inorg. Chem*., 2016, 1748–1755; (c) C. Huang, S. Du, G. A. Solan, Y. Sun, W.-H. Sun, *Dalton Trans*., 2017, 46, 6948–6957.
14. (a) F. Huang, W. Zhang, Y. Sun, X. Hu, G. A. Solan, W.-H. Sun, *New J. Chem*., 2016, 40, 8012–8023; (b) Y. Zhang, H. Suo, F. Huang, T. Liang, X. Hu, W.-H. Sun, *J. Polym. Sci, Part A: Polym. Chem*., 2017, 55, 830–842.
15. (a) J. Ba, S. Du, E. Yue, X. Hu, Z. Flisak, W.-H. Sun, *RSC Adv*., 2015, 5, 32720–32729; (b) F. Ragani, M. Gasperini, E. Gallo, P. Macchi, *Chem. Commun*., 2005, 1031–1033.
16. (a) S. Fernandes, R. M. Bellabarba, A. FG. Ribeiro, P.T. Gomes, J. R. Ascenso, J. F. Mano, A. R. Dias, M. M. Marques, *Polym. Int*., 2002, 51, 1301–1303; (b) S.-Y. Jie, W.-H. Sun, T. Xiao, *Chinese Journal of Polymer Science*., 2010, 3, 299–304; (c) J. Ma, C. Feng, S. Wang, K.-Q. Zhao, W.-H. Sun, C. Redshaw, G. A. Solan, *Inorg. Chem. Front*., 2014, 1, 14–34.
17. F. A. R. Kaul, G. T. Puchta, G. D. Frey, E. Herdtweck, W. A. Herrmann, *Organometallics*, 2007, 26, 988–999.
18. (a) W.-H. Sun, X. Tang, T. Gao, B. Wu, W. Zhang, H. Ma, *Organometallics*, 2004, 23, 5037–5047; (b) V. C. Gibson, C. Redshaw, G. A. Solan, A. J. P. White, D. J. Williams, *Organometallics*, 2007, 26, 5119–5123.

19. (a) V. C. Gibson, S. McTavish, C. Redshaw, G. A. Solan, A. J. P. White, *Dalton Trans*., 2003, 221–226; (b) R. K. O'Reilly, V. C. Gibson, A. J. P. White, D. J. Williams, *Polyhedron*, 2004, 23, 2921–2928; (c) V. C. Gibson, N. J. Long, P. J. Oxford, A. J. P. White, D. J. Williams, *Organometallics*, 2006, 25, 1932–1939.
20. (a) R. P. Thummel, Y. Jahng, *J. Org. Chem*., 1985, 50, 2407–2412; (b) R. P. Thummel, F. Lefoulon, D. Cantu, R. Mahadevan, *J. Org. Chem*., 1984, 49, 2208–2212; (c) S. Meiries, K. Speck, B. D. Cordes, A. M. Z. Slawin, S. P. Nolan, *Organometallics*, 2013, 32, 330–339; (d) Q. Mahmood, Y. Zheng, X. Wang, Y. Sun, W.-H. Sun, *Dalton Trans*., 2017, 46, 6934–6947.
21. G. M. Sheldrick, SHELXTL-97, *Program for the Refinement of Crystal Structures*; University of Gottingen, Göttingen, Germany, 1997.
22. L. Spek, *Acta Crystallogr., Sect. D: Biol. Crystallogr*., 2009, 65, 148–155.
23. (a) A. W. Addison, T. N. Rao, *J. Chem. Soc. Dalton Trans*., 1984, 1349–1356; (b) J. Yuan, W.-B. Shi, H.-Z. Kou, *Transition. Met. Chem*., 2015, 40, 807–811.
24. T. Xiao, S. Zhang. G. Kehr, X. Hao, W.-H. Sun, *Organometallics*, 2011, 30, 3658–3666.
25. N. V. Semikolenova, W.-H. Sun, I. E. Soshnikov, M. A, Matsko, O. V. Kolesova, V. A. Zakharov, K. P. Bryliakov, ACS Catal., 2017, 7, 2868–2877.

GRAPHICAL ABSTRACT

CHANTSALNYAM BARIASHIR, ZHENG WANG, SHIZHEN DU, GREGORY A. SOLAN,* CHUANBING HUANG, TONGLING LIANG, WEN-HUA SUN*

Cycloheptyl-fused N,N,O-ligands as electronically modifiable supports for M(II) (M = Co, Fe) chloride pre-catalysts; probing performance in ethylene oligo-/polymerization

Cobalt (II) and iron (II) chloride complexes bearing N,N,O-α-imino-α'-oxo-2,3:5,6-bis(pentamethylene)pyridines, have been assessed a pre-catalysts in ethylene oligo-polymerization. Upon activation with MMAO the Fe-prectalysts exhibited good activity for ethylene polymerization forming linear low molecular weight polymers while **Co**/MMAO showed high activity for ethylene oligomerization produced short chain ethylene oligomers with good α-olefin selectivity.